

Video Article

Membrane Transport Processes Analyzed by a Highly Parallel Nanopore Chip System at Single Protein Resolution

Michael Urban¹, Marc Vor der Brüggen², Robert Tampé¹

¹Institute of Biochemistry, Biocenter, Goethe University Frankfurt

²Nanospot GmbH

Correspondence to: Robert Tampé at tampe@em.uni-frankfurt.de

URL: <https://www.jove.com/video/53373>

DOI: [doi:10.3791/53373](https://doi.org/10.3791/53373)

Keywords: Biophysics, Issue 114, model lipid bilayers, pore-spanning membrane, nanopores, suspended bilayer, lab-on-chip, biosensor, membrane transport, membrane proteins, array, membranes

Date Published: 8/16/2016

Citation: Urban, M., Vor der Brüggen, M., Tampé, R. Membrane Transport Processes Analyzed by a Highly Parallel Nanopore Chip System at Single Protein Resolution. *J. Vis. Exp.* (114), e53373, doi:10.3791/53373 (2016).

Abstract

Membrane protein transport on the single protein level still evades detailed analysis, if the substrate translocated is non-electrogenic. Considerable efforts have been made in this field, but techniques enabling automated high-throughput transport analysis in combination with solvent-free lipid bilayer techniques required for the analysis of membrane transporters are rare. This class of transporters however is crucial in cell homeostasis and therefore a key target in drug development and methodologies to gain new insights desperately needed.

The here presented manuscript describes the establishment and handling of a novel biochip for the analysis of membrane protein mediated transport processes at single transporter resolution. The biochip is composed of microcavities enclosed by nanopores that is highly parallel in its design and can be produced in industrial grade and quantity. Protein-harboring liposomes can directly be applied to the chip surface forming self-assembled pore-spanning lipid bilayers using SSM-techniques (solid supported lipid membranes). Pore-spanning parts of the membrane are freestanding, providing the interface for substrate translocation into or out of the cavity space, which can be followed by multi-spectral fluorescent readout in real-time. The establishment of standard operating procedures (SOPs) allows the straightforward establishment of protein-harboring lipid bilayers on the chip surface of virtually every membrane protein that can be reconstituted functionally. The sole prerequisite is the establishment of a fluorescent read-out system for non-electrogenic transport substrates.

High-content screening applications are accomplishable by the use of automated inverted fluorescent microscopes recording multiple chips in parallel. Large data sets can be analyzed using the freely available custom-designed analysis software. Three-color multi spectral fluorescent read-out furthermore allows for unbiased data discrimination into different event classes, eliminating false positive results.

The chip technology is currently based on SiO₂ surfaces, but further functionalization using gold-coated chip surfaces is also possible.

Video Link

The video component of this article can be found at <https://www.jove.com/video/53373/>

Introduction

The analysis of membrane proteins has become of increasing interest for basic and pharmaceutical research in the past 20 years. The development of novel drugs depends on the identification and detailed characterization of new targets, currently being one of the limiting factors. The fact that about 60% of all drug targets are membrane proteins¹, makes the development of techniques to elucidate their function most important.

In the past, techniques for the study of electrogenic channels and transporters have been developed in multitude²⁻⁴. Non-electrogenic substrates in contrary present a more challenging task. They are however of special interest as prime drug targets, as they control the flux of solutes and nutrients across the cell membrane and function as key receptors in signaling cascades⁵.

Considerable effort has been put into the development of techniques to study the function of membrane transport proteins^{6,7}. Systems using solid-supported membranes have emerged as most promising tools in this field⁸⁻¹⁰, including solid supported lipid bilayers, tethered bilayers^{11,12}, microblack lipid membranes^{13,14} and native vesicle arrays^{15,16} to name a few. Some of them are even available as commercial setups^{17,18}. Some examples have been published combining the ability to study single membrane proteins in a highly parallel manner^{14,19}, a prerequisite for screening applications. However, these methods rarely bridge from basic research to the industrial environment. The difficulties often lie in the ability of the system to be automatable, the cost-intensive production and/or laborious preparation. An approach overcoming all the above mentioned obstacles is the final aim.

The technique presented here was developed to study membrane channels and transporters *in vitro* in a controlled environment on the single protein level²⁰⁻²². Reconstitution of purified membrane proteins into LUVs is much more established than comparable approaches for GUVs²³⁻²⁶.

or black lipid membranes²⁷. They can directly be applied to the chip surface, where bilayer formation is taking place via a self-assembly process. The glass-bottom design of the nanoporous chip (**Fig. 1**) allows for air microscopy, which permits the straightforward automation of the system. In combination with a motorized stage multiple chips can be measured at the same time, with each field of view containing thousands of sealed cavities for analysis.

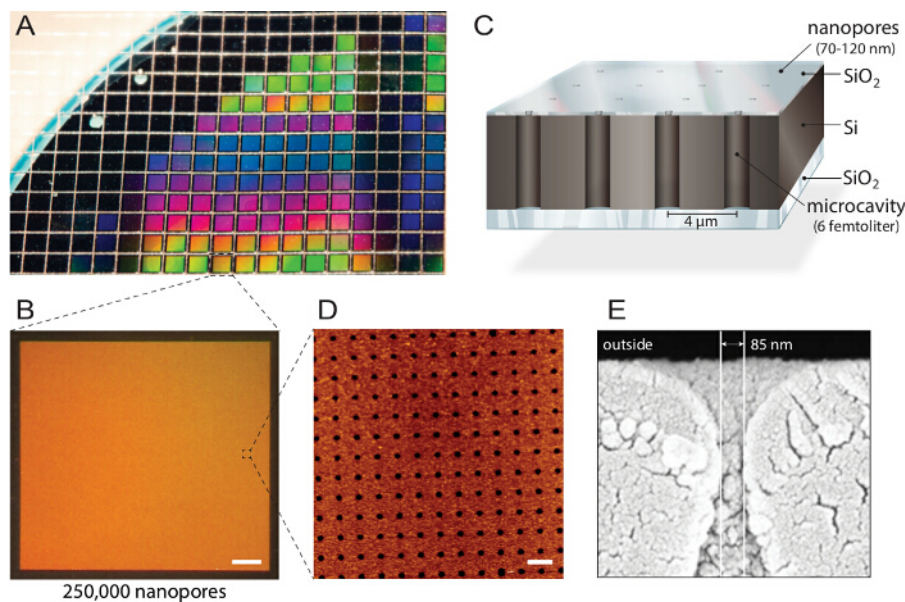


Figure 1. Design of multiplexed nanopore biochips. **A)** A silicon-on-insulator (SOI) wafer is structured by reactive-ion etching. Approximately 1,150 individual chips are fabricated from each wafer with identical properties and quality. **B)** Each chip comprises 250,000 individual microcavities with nano apertures. Scale bar: 200 μm . **C)** Each cavity is addressable via multi-spectral fluorescence read-out. An intransparent top layer blocks the fluorescent signals from the buffer reservoir, making the biochip compatible with inverted fluorescence microscopes. **D)** Atomic force microscopy (AFM) imaging reveals evenly arranged pore openings and surface roughness of the silicon dioxide layer of 3.6 nm ($n = 40$) optimal for vesicle fusion. Scale bar: 5 μm . **E)** Scanning electron microscopy (SEM) image shows a cross-section through the nanopore allowing access to the femtoliter cavities inside the silicon chip. This figure was reused with permission from ²¹. [Please click here to view a larger version of this figure.](#)

All data analysis is performed using freeware to guarantee unrestricted access for end users. Time series are analyzed using free image processing software and a custom build curve analysis software enabling batch processing and straightforward correlation of large datasets with multiple fluorescent channels and thousands of curves.

The model protein used in this protocol is the mechanosensitive channel of large conductance (MscL) channel protein derived from *E. coli*. It functions as a valve to release osmotic shock in nature, but was modified in such a way that rationally designed synthetic functionalities can covalently be attached to the channels constriction side. Via charge-repulsion of the covalently bound activator (MTSET) the channel is triggered to open, creating a nano-valve. Small molecules like ions, water, small proteins, but also small fluorophores can permeate through the channel. Here, the protein is used as a model to demonstrate the ability of the system to detect protein-mediated translocation.

Protocol

1. Preparation of Large Unilamellar Vesicles (LUVs)

- Clean a round bottom flask (10 ml volume) with nitrogen gas to remove any dust particles. Rinse the round bottom flask with ethanol.
Note: Residual ethanol can be tolerated and does not disturb subsequent steps.
- Wash a 1 ml glass syringe 4x with chloroform, to remove any contamination. Add 4 ml SoyPC20 (25 mg/ml in chloroform) to the round bottom flask and dope the lipid solution with an additional DOPE^{ATTO390} to a final concentration of 0.1 mol%.
Note: Instead of DOPE^{ATTO390} other fluorophore-labeled lipids or lipophilic dyes can also be used, depending on available excitation sources.
- Connect the round bottom flask to a rotary evaporator. Dry the lipid film for 40 min at 300 mbar, 30 °C water bath temperature and maximal rotation speed, to form a homogenous lipid film on the glass wall of the flask.
- Transfer the flask to a high vacuum pump and dry the lipid film for additional 30 min at room temperature.
- Add 5 ml buffer (20 mM Tris, 150 mM NaCl, pH 8.0; sterile filtered) and 8 glass beads (2.7-mm diameter, ethanol washed and dried) to the flask. Connect the flask to the rotary evaporator and rotate without vacuum at 50 °C at maximum speed.
Note: Glass beads mechanically displace the lipid film from the glass wall, leading to (multilamellar) vesicle formation. After 45 min rotation the solution appears milky and no residual lipid film should be visible at the flask walls. Instead of glass beads other methods like sonicating the flask in a water bath sonifier, vortexing the flask or the gentle rehydration method are also applicable.
- Transfer the flask under inert gas (argon) to an ultrasonic bath and sonicate for 4 min at room temperature.
Note: The ultrasound shockwaves disrupt the liposomes, making them unilamellar.
- Split the LUV solution into 1 ml aliquots.
- Perform 5 freeze/thaw cycles by freezing the LUV solution in liquid nitrogen, followed by thawing at 40 °C in a water bath.

Note: This leads to rupture and spontaneous rearrangement of individual liposomes with each other, leading to size increase.

9. At the last freezing step store all samples at -80 °C.

Note: The LUVs will be stable for at least 6 months.

2. Protein Reconstitution

1. Thaw 1 ml LUV aliquot on ice. Directly before reconstitution, extrude liposomes 17x through a 400 nm polycarbonate filter membrane using a mini extruder.
Note: Lipid aggregates will be removed and the final homogenous size distribution is reached.
2. Destabilize LUVs by addition of 4% Triton X-100 (v/v) to a final concentration of 0.25% (v/v) and incubate for 5 min at 50 °C.
Note: The amount of liposomes used in this step depends on the mass of the purified MscL^{G22C} used (see step 2.3). Purify MscL^{G22C} (derived from *E. coli*) as described in detail in²⁸.
3. Mix purified MscL^{G22C} and detergent-saturated liposomes at 1:20 (w/w) ratio and incubate for additional 30 min at 50 °C.
4. For detergent removal add bio-beads in Tris buffer (20 mM Tris, 150 mM NaCl, pH 8.0; sterile filtered) to the protein/liposome solution, with 16 mg (wet weight) bio-beads per μ l detergent used to destabilize liposomes in step 2.2.
5. Perform detergent removal overnight (16 hr) at 4 °C on a rotating plate.
Note: The constant mixing of the solution ensures optimal detergent removal.
6. After detergent removal store proteoliposomes at 4 °C and use for experiments on the same day.

3. Activity Assay

1. During protein reconstitution take a 100 μ l aliquot of detergent-destabilized proteoliposome solution after finishing step 2.3.
2. Add 1 volume of calcein (30 mM) to the protein-liposome solution and incubate additional 5 min at 50 °C.
3. Remove detergent from the solution as described in step 2.4 - 2.6.
4. After detergent removal equilibrate a size-exclusion column (20 ml bed volume or more) with Tris buffer (3x the bed volume).
Note: Proteoliposome separation can be performed at room temperature, however keeping the sample constantly at 4 °C is advised to ensure best protein activity after fractionation.
5. Separate proteoliposomes from free calcein by applying the entire aliquot (200 μ l) to the size exclusion column. Allow the mixture to soak into the column, followed by elution of the proteoliposomes from the column via continuous buffer application on top using gravity flow. Observe the calcein containing proteoliposomes as a discrete orange band in the elution front. Collect fractions of 500 μ l respectively.
Note: Free calcein dye will elute after the proteoliposome fraction with complete separation.
6. Pipette 80 μ l of each fraction onto a micro-well plate for fluorescent read-out and identify the fraction containing the highest amount of calcein containing proteoliposomes via fluorescence emission. Detect fluorescence at 520 nm with excitation at 490 nm. Use the proteoliposome fraction with the highest signal for the following activity assay.
7. Mix 20 μ l of the proteoliposome-containing fraction with 980 μ l Tris buffer in a 1 ml fluorescence cuvette.
8. Measure fluorescence emission at 520 nm (excitation 490 nm) using a spectrofluorometer. Record for 1 min and then add 25 μ l of MTSET ([2-(trimethylammonium)ethyl]methanethiosulfonate) from a stock solution (160 mM) and mix well. Keep on recording during mixing. Always prepare the stock solution fresh directly before use.
Note: Once solved in buffer MTSET hydrolyzes within 30 min and will be non-reactive. MTSET can be weighed and kept as dry powder aliquot at -20 °C until use.
Note: Once activated the MscL^{G22C} channel opens and releases the entrapped calcein, leading to a local concentration decrease of the calcein when effluxing the proteoliposomes and subsequent dequenching of the dye, resulting in an increase of the fluorescence emission.
9. After the fluorescence emission has reached a stable plateau again, solubilize the liposomes by addition of 50 μ l Triton X-100 (4% v/v).
Note: Ideally no further fluorescence increase can be observed, implying active protein in every liposome.

4. Size Distribution Measurement of LUVs Using Nano-particle Tracking

1. Note that only minimal samples of the liposome or proteoliposome solution are necessary for size distribution analysis using the nanoparticle tracker. Dilute a liposome solution of 5 mg/ml lipid concentration 1:5,000 (v/v) in buffer (20 mM Tris, 150 mM NaCl, pH 8.0; sterile filtered) for analysis to a final volume of 1 ml. Filter all buffers used for dilution and prior LUV preparation and reconstitution using a 0.2 μ m membrane to remove any suspended particles like dust that would disturb size distribution measurements.
2. Wash the flow-chamber with ultra-pure water.
3. Use the surface markers to focus on the light beam. Inject approximately 300 μ l of the diluted liposome sample and immediately close the exit valve to stop the flow inside the flow chamber, without introducing any air bubbles.
4. Adjust focus and camera shutter/gain settings to ensure adequate scattering signal of the sample for detection.
Note: 20 - 80 signals should be clearly visible in the field of view. Prevent overcrowding (> 80 signals) as the software will not be able to track individual signals when overlapping.
5. Go to the "Capture" screen. Adjust the temperature control to 25 °C and the capture duration to 90 sec using the software controls. Press "Record" to start recording a time series.
Note: Upon completion of the time series a new window opens.
6. Save the time series in the given format (*.avi). For practical reasons during batch analysis save all files in a single folder.
7. Open the exit valve and inject another 300 μ l into the flow chamber. Close the valve and repeat steps 4.3 - 4.6 twice.
8. After completing all sample runs wash the flow chamber with 5 ml ultra-pure water. Go to the "Pre-Process" screen. Set the calibration parameters temperature = 25 °C and viscosity = 0.91 for the Tris buffer used in this protocol.
9. Open the batch process window and load the recorded time series (Advanced/Batch Process/Set File 1-3). Press "GO" to start the size distribution analysis.
Note: the analytical software automatically tracks the single particles and calculates their diameter based on their movement behavior using the parameters set in step 4.8.

Note: The resulting size distribution analysis saves automatically into the same folder as the time series files.

10. Additionally create a report file to summarize the results (Export/Create Report PDF).

5. Chip Holder Preparation

1. Weigh 1.0 g of MDX4 medical grade elastomer base and 0.1 g MDX4 curing agent into a 50 ml reaction tube. Blend both thoroughly with a glass bar.
2. Put the tube into a desiccator for 1 hr to degas the adhesive. Afterwards use it within 30 min for chip gluing, as the adhesive will harden and be too hard to work with.
3. During elastomer degassing (step 5.1) clean an objective glass slide thoroughly with chloroform to remove any contaminations before chip bonding. Rinse the slide with 5 ml of chloroform using a glass syringe. Collect the chloroform in an underneath positioned beaker. After washing let the slide dry.
Note: Perform this step under a fume hood. Alternative to chloroform, other organic solvents like acetone can also be used.
4. Deposit a small amount of the adhesive bonding material onto the cover glass using a pipette tip (crystal tips for 10 μ l pipettes). Remember that the chips have to fit into the 8-chamber slide holder later on and have to be placed on the slide accordingly.
5. Carefully remove one chip at a time from the wafer board using fine tip tweezers and deposit the chip on the drop of adhesive on the cover glass. Ensure that the coated side of the chip faces upwards.
6. Gently push the chip onto the cover glass with the back of a blunt PE tweezers. To ensure that the glue is dispensed evenly underneath the chip, carefully slide the chip forth and back. **CRITICAL STEP:** Ensure that no air bubbles are trapped underneath the chip, as it will disturb optical imaging of the chip cavities later on. Also ensure that no adhesive material contaminates the chip surface.
7. Desiccate the finished cover glass for 2 hr at 65 °C in a cabinet dryer.
Note: Chips are still coated with a protective layer originating from their fabrication that needs to be removed.
8. To remove the protective layer, perform a sequential solvent washing step. During the curing of chips, preheat a water bath to 54 °C.
9. Place 3 glass beakers into the water bath, two of them filled with isopropanol and one filled with acetone.
10. Insert the chip cover glass into a slide holder and submerge it into the first isopropanol filled dish for 10 min. Afterwards transfer it to the acetone filled dish, incubate again for 10 min before transferring it for the final washing step to the second isopropanol dish and incubate another 10 min.
11. Remove the slide holder from the dish and carefully wash it extensively with ultrapure water, followed by drying the chips with a gentle stream of nitrogen gas.
12. Take-off the lamination sheet from the 8-well sticky-slide and put it backwards on the bench. Carefully pick up the cover slide and gently press onto the sticky-slide with the chips facing the wells. Let the finished chip holder rest for a couple of minutes before use.

6. Assay Preparation

Note: Nanopore chips glued to a cover glass and separated by an 8-well sticky-slide possess the benefit, that multiple chips can be addressed in a single experimental run, with chips being completely separated from each other.

1. After chip holder preparation, rinse each chip with pure ethanol and blow dry with nitrogen gas, to remove any contaminations like dust.
2. Clean the chip surface with air, oxygen or nitrogen plasma. Depending on the type of plasma cleaning time-periods vary: perform oxygen plasma treatment for 1 min, air and nitrogen plasma for 5 min at 0.3 mbar at 80% power setting (RF power medium or high).
3. After plasma cleaning incubate chips in pure ethanol for 10-15 min to ensure cavity wetting.
4. Stepwise exchange ethanol for buffer by adding 400 μ l of Tris buffer (20 mM Tris, 150 mM NaCl, pH 8.0; sterile filtered), followed by mixing of the solution without introducing air bubbles and subsequent removal of 400 μ l. Repeat this procedure 12 times, to ensure ethanol removal.
Note: Ethanol would be harmful for liposomes and suspended lipid bilayers.
5. Dope Tris buffer (20 mM Tris, 150 mM NaCl, pH 8.0; sterile filtered) with 5 mM CaCl_2 and 1 μ M Oy647 dye. Completely remove the washing buffer from the chip and immediately add the doped buffer to the chip. **Note:** Chips will be covered with a thin buffer film after wash buffer removal, so the chip is not in direct contact with air, ensuring a constant wetting of the cavities and the chip surface.
6. Add 1 mg/ml LUVs or proteo-LUVs in Tris buffer (20 mM Tris, 150 mM NaCl, pH 8.0; sterile filtered) to each well.
Note: The final volume in each well is 300 μ l. Consider subsequent additions of the control dye and the chemical modifier MTSET during doped Tris buffer addition.
7. For pore-spanning lipid bilayer formation on the chip surface incubate the chip for 1 hr at room temperature with the liposome solution. Afterwards wash each chip with 4x 400 μ l of Ca^{2+} -free Tris buffer.
8. Add the control dye to each well, with a final concentration of 5 μ M. The chips are now ready for the translocation assay.

7. Assay Setup

1. Mount the chip holder to the epifluorescence microscope (20X air objective, long working distance). Focus on the rim of the nanopore chip to more easily find the focal plane of the micro-cavities. Once the cavities are in focus scan the nanopore array for a region that displays highest sealing ratio.
Note: Every inverted epifluorescence microscope can be used to perform chip assays. Depending on the objective magnification (20X - 60X) the number of assayed cavities will vary, with up to 9,000 cavities in a single field of view using 20X magnification. Air objectives with a long working distance are preferable. The use of inverted confocal laser scanning microscopes (CLSM) is also possible, but image acquisition might be the limiting factor due to the limited depth of focus.
2. Optimize the chip illumination.
Note: Ensure that both dye channels do not exceed the maximum grey scale value, as changes cannot be observed. For export experiments adjust illumination of the translocated dye to 90% of maximum signal capacity. Adjust the control dye in open cavities to 80-90% of maximum signal capacity to clearly detect any leaky membrane sealing.
3. Once all channels are adjusted start the time series. Take images every 10-20 sec for 90 min.

Note: This is adequate to likewise follow specific and unspecific efflux events.

4. Initialize efflux of the fluorescent substrate by the addition of cysteine-specific, positively charged compound MTSET to a final concentration of 3 mM. Allow at least 5 min of experiment runtime before MTSET addition to be able to later on establish a stable fluorescent signal baseline prior to channel opening. Always prepare MTSET solution fresh directly before usage.

8. Data Analysis

1. Open the time series image stack with a standard version of ImageJ (File/Import/Image Sequence).
2. If fluorescent channels are stacked, split the channels in individual stacks for each channel (Image/Stacks/Stack to Images).
3. Duplicate the first image of the translocation substrate channel for ROI (regions of interest) identification (Image/Duplicate).
4. Convert the image to a binary image (Image/Adjust/Threshold). Ensure that the algorithm used depicts signals for all sealed cavities without overlapping pixilation.
5. Automatically define regions of interest with the particle analyzer tool (Analyze/Analyze Particle). Define a minimum particle size defined, to avoid particle noise. Check the options "exclude on edges" and "include holes". Ensure that resulting ROIs reflect the microcavity array pattern. Interjacent ROIs are artifacts, therefore remove them. Save the ROI list.
Note: Measurement parameter has to be set to "area" before particle analysis (Analyze/Set Measurements/Area)
6. Open the Time Series Analyzer plug-in (<http://rsb.info.nih.gov/ij/plugins/time-series.html>), which resizes all ROIs automatically to the same size. Re-size all existing ROIs to a width/height of 6x6 pixels and oval shape (Timer Series Analyzer/AutoROIProperties). Check the option "Resize existing ROIS". Save the resulting resized ROI list.
7. Open the ROI manager (Analyze/Tools/ROI Manager) and load the resized ROI list for each channel of the time series (ROI Manger/More/Open). ROIs will be superposed. To analyze the signal change for each ROI start the Multi Measure tool (ROI Manager/More/Multi Measure), select "Measure all slices" and "One row per slice" and start the multi measure.
Note: Measurement parameter has to be set to "mean gray value" for this step (Analyze/Set Measurements/Mean gray value)
8. Save the resulting table, giving the mean grey value for each ROI in *.txt or *.xls format.
9. Import the ROI analysis of each imaging channel into NanoCalcFX via the "Import File" option. Set "Use first line for naming series". Set the step size between images according to the time series image acquisition periods and choose the corresponding column and decimal separator.
10. Use the "multiple sheet" option to automatically correlate the graphs of the individual fluorescent channels.
Note: The events can now be analyzed and classified using the information given by the 3-color spectral information.
11. Fit selected curves using the build-in fit function (fit option).
Note: The implemented efflux and influx equation is suitable for all monoexponential diffusion-driven events and fit boundaries can be set. Resulting rate constants can be plotted using the histogram tool or exported for further data refinement.

Representative Results

Pore-spanning membranes can easily be created on the nanostructured chip surface in a self-assembled manner. However the underlying process is still delicate and influenced by many parameters like liposome size, monodispersity of the liposome population, lamellarity, lipid- and salt-concentration and chemical surface properties. Most of these parameters have been carefully characterized and standardized in the above protocol. Other parameters however should be checked during every new preparation, to ensure a successful experiment. These are the liposome size distribution and population dispersity (**Fig. 2A**). For optimal pore-spanning membrane formation and to avoid liposome intrusion into the cavity space liposome sizes well above the pore diameter are a necessity. Furthermore, monodisperse liposome preparations have been shown to yield best results in membrane spreading and fusion. Another crucial step that has to be checked for every preparation is protein activity after reconstitution. Using a fluorescence-dequenching assay for liposomes reconstituted with MscL^{G22C}, channel opening can be monitored via fluorescence spectroscopy, giving a ratio of liposomes harboring active MscL^{G22C} protein (**Fig. 2B**).

Once spread to the chip surface, solute translocation of a fluorescent target by MscL^{G22C} upon ligand activation can be followed (**Fig. 3B**). Engineered MscL^{G22C} channels are closed in their default state, entrapping small fluorescent molecules inside the cavity space. By addition of the chemical modulator MTSET positive charges are introduced to the constriction region of the MscL^{G22C} pore, pushing it open via electrostatic repulsion. The prior entrapped fluorophore evades the cavity space to achieve diffusion equilibrium. The subsequent decrease of fluorescence inside the cavity space can be monitored. This process is highly reproducible, resulting in a homogenous population of efflux events (**Fig. 3C**). The resulting efflux curves cluster in two distinct populations, demonstrating the ability of the assay to discriminate between single- and multichannel translocation events (**Fig. 3D**). Furthermore the system is able to follow up to three spectrally well separated dyes in parallel and in real-time, making it possible to record high-content screenings and discriminate precisely and objectively between positive, false positive and negative results. In this study 9.046 sealed cavities were analyzed, of which 8% displayed efflux behavior. Deploying the different fluorescent read-out channels, events can be discriminated into monoexponential efflux events, complex kinetics, lipid intrusions and membrane ruptures (**Fig. 3E**). Only events that display steady signals for the control solute and the membrane dye are considered for final analysis. Complex kinetics represent efflux events with unsteady control signals and are therefore omitted. Lipid intrusions and membrane ruptures are artifact events intrinsically occurring using pore-spanning lipid bilayer systems. They can be discarded using the control dye signals as mentioned above (**Fig. 4**).

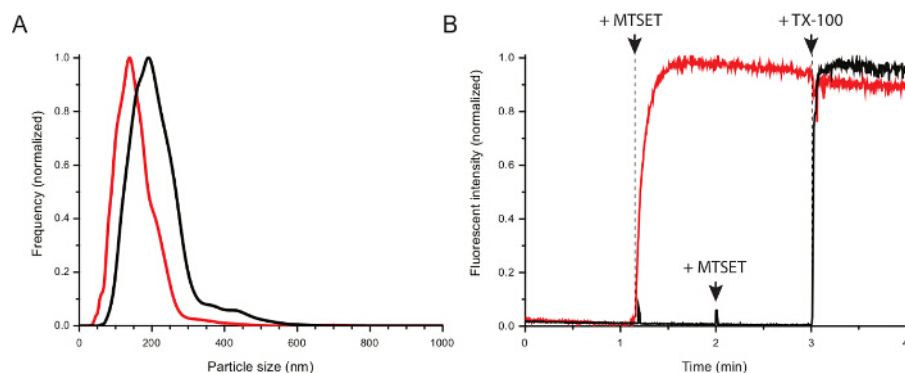


Figure 2. Size distribution of proteoliposomes and MscL function. **A)** Vesicles were analyzed by nano-particle tracking analysis. LUV samples were examined before (black trace) and after reconstitution of MscL^{G22C} (red trace). After LUV preparation, a mean particle size of 214 ± 70 nm is achieved. The size is decreased during reconstitution, resulting in proteoliposomes of 158 ± 60 nm in size. **B)** MscL activity was validated after reconstitution by an efflux assay.²⁸ Self-quenched calcein is released from proteoliposomes through MTSET-mediated opening of the MscL channel, leading to dequenching of the fluorophore (red) and a rapid increase of the fluorescence intensity. Liposomes without protein show no such efflux, even after repeated MTSET addition (black). Subsequent detergent-introduced solubilization (TX-100) of the liposomes releases all previously encapsulated dye. This figure was reused with permission from²¹. [Please click here to view a larger version of this figure.](#)

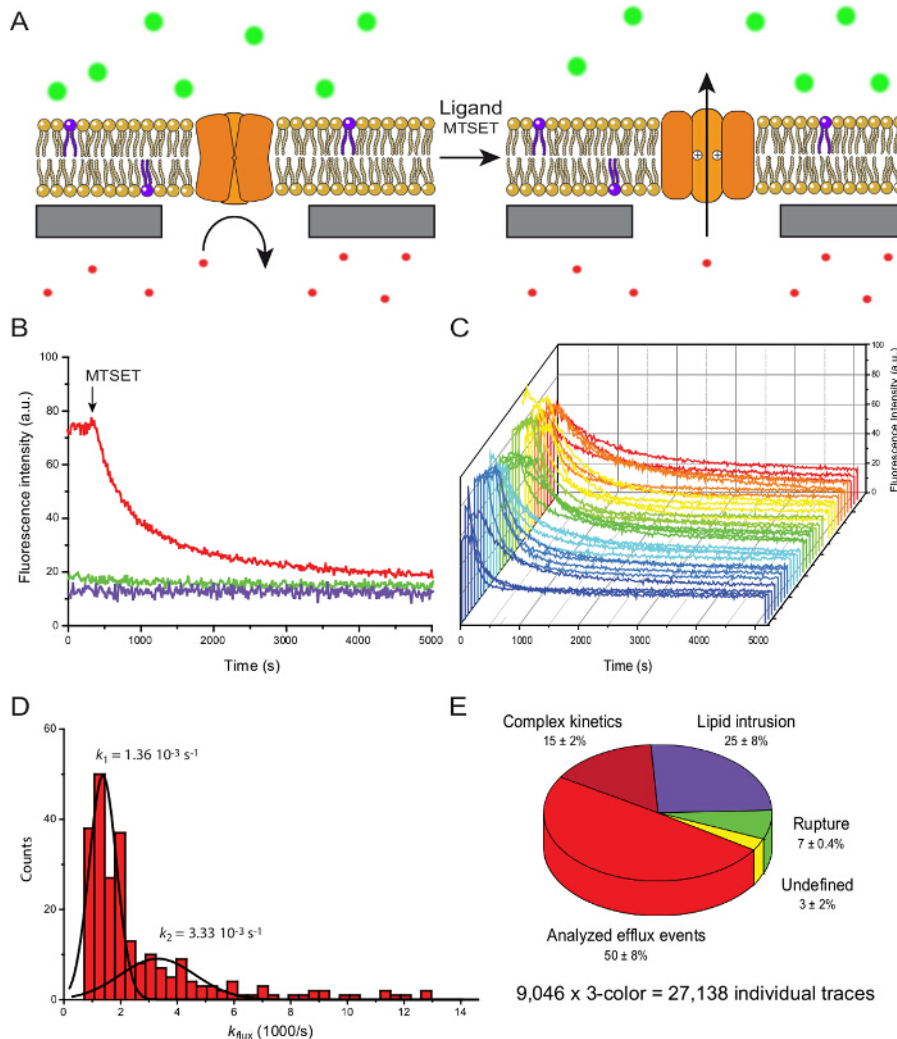


Figure 3. Ligand-gated solute translocation by MscL at single-molecule level. **A)** Engineered MscL^{G22C} channels are closed in their default state. Small solutes such as a fluorophore are unable to pass neither through the channel nor the lipid bilayer. Upon addition of MTSET, an engineered single cysteine of each MscL^{G22C} protomer gets modified, introducing multiple positive charges in the constriction side of the pentameric channel complex. The MscL^{G22C} channel is pushed open by charge repulsion and the entrapped dye can diffuse out of the cavity, leading to a decrease in fluorescence intensity. **B)** Time traces of MscL^{G22C} opening upon addition of MTSET. Proteoliposomes containing functionally reconstituted MscL^{G22C} were spread on the chip surface. Oy647 (red) was entrapped inside the cavities as translocation substrate. OregonGreen Dextran (70 kDa, green) was added as channel impermeable control substrate to monitor the substrate specificity of the transport event as well as the membrane integrity during the experiment. LUVs were supplemented with DOPE^{ATTO390} (0.1 mol%; purple) to check for lipid contamination inside cavities. Addition of MTSET (3 mM final) at t = 0 sec opens the channel, leading to Oy647 efflux from the cavities, recorded via fluorescence read-out. **C)** Randomly picked MscL^{G22C} efflux curves demonstrate typical efflux events. **D)** Rate constants for translocation events (n = 242) cluster into two Gaussian populations, demonstrating that single- and multi-channel transport events can be discriminated. **E)** High-content screening and statistical analysis of 9,046 sealed chip cavities by triple-color real-time readout. 8% of all analyzed chip cavities show exponential efflux events. Due to spectral decoding (red: translocated solute; green: control solute; violet: lipid), efflux events, complex kinetics, lipid intrusions, and membrane ruptures could be discriminated, thus eliminating false positives. This figure was reused with permission from ²¹. [Please click here to view a larger version of this figure.](#)

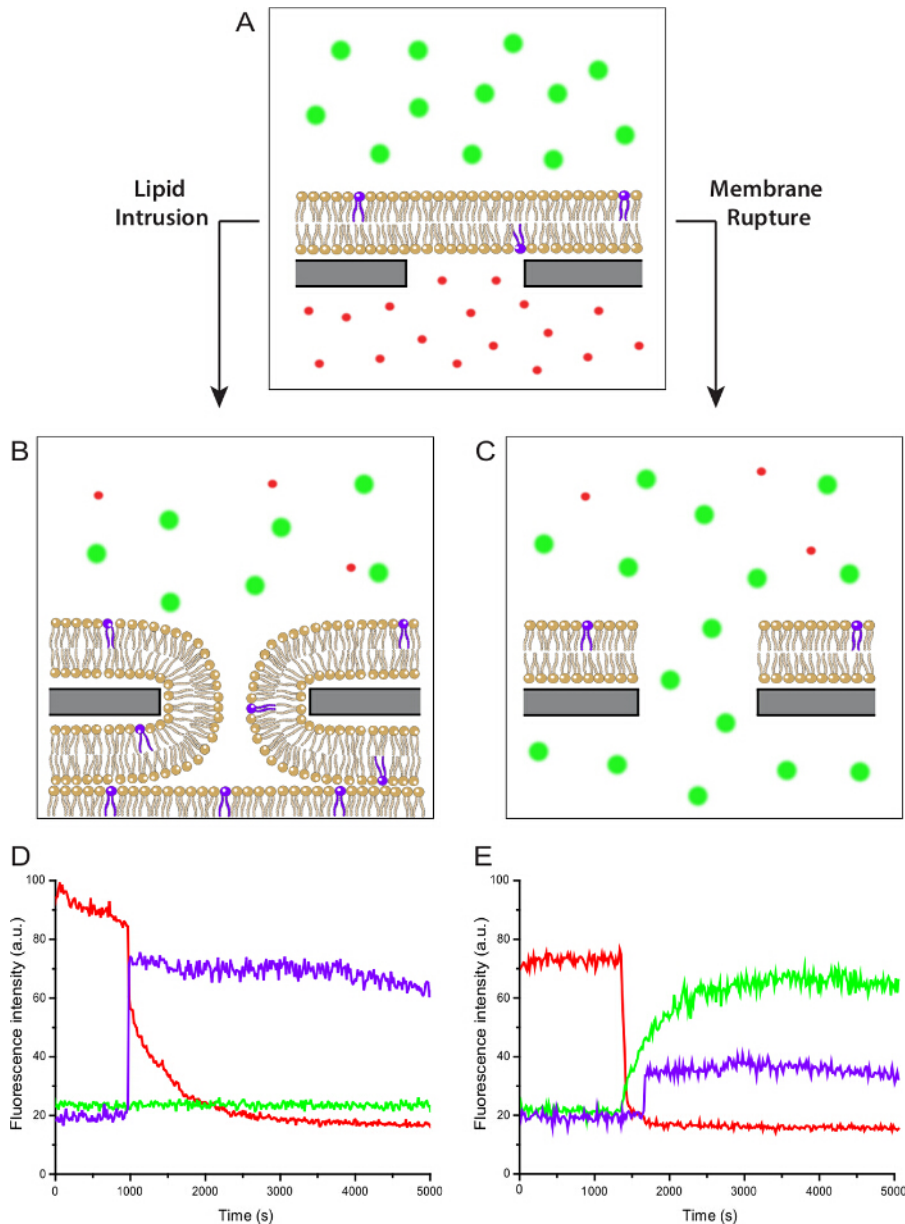


Figure 4. Event classes distinguished by three-color detection. Translocated solute (red), control solute (green) and a lipid dye (violet) can be spectrally discriminated allowing for unbiased data selection. **A)** Sealed cavities harboring no membrane protein show no flux events under the experimental conditions described for the MscL channel recording (see **Fig. 3A**). The fluorescent readout is stable for all channels. **B)** Ill-defined suspended lipid bilayers are able to intrude the cavity. **C)** Membrane rupture results in discontinuous lipid bilayer spanning the nanopore fissures. Thereby, the cavity space is no longer separated from the buffer compartment. Entrapped dyes (red) evade the cavity down the concentration gradient. The control solute (green), previously unable to pass across the membrane, enters the cavity. **D)** Example for a lipid intrusion event. While the fluorescent signal for the lipid dye (violet) increases due to the membrane invading the cavity space, the translocation solute is pushed out of the cavity (red), leading to a decrease in fluorescent signal. The nanopore is blocked by the lipid bilayer, preventing the passage of the control substrate (green). **E)** During membrane rupture, the enclosed transport solute rapidly evades from the cavity (red), while the control solute diffuses in (green). This figure was reused with permission from ²¹. [Please click here to view a larger version of this figure.](#)

Discussion

The technique presented here allows a highly parallel analysis of membrane protein transport. Reconstituted membrane protein systems can directly be applied to the biochip, making the adaption of theoretically every membrane transporter or channel possible. Transport analysis is only limited by the establishment of a fluorescent read-out system, either via direct fluorescence change (translocation of fluorophores or fluorescently labeled substrates) or indirect fluorescence change (pH-sensitive dyes, secondary enzymatic reactions). The latter, however have yet to be established.

Functional characterization of membrane channels or transporters on the single protein level is the main focus of this technique. In combination with an automated microscope, the establishment of screening applications for protein effectors is also possible. The assay setup allows the

parallel recording of up to 8 chips, with multiple assay points on each chip. Because of complete separation of the chips, it is truly parallel, allowing for multiple experimental repeats including controls in a single experimental run, once the conditions have been established.

Critical steps during setting up an experiment are the preparation of truly unilamellar vesicles, the active reconstitution of the protein of choice, spreading efficiency of proteoliposomes on the chip surface and the retention capability of the suspended lipid bilayer toward the substrates used in the assay.

While the preparation of unilamellar vesicles is of basic importance for this assay to avoid the establishment of multilamellar membrane sheets on the chip surface during suspended lipid bilayer formation, it is rather easy to ensure unilamellarity of the vesicles via sonicating the liposomes during preparation.

The direct application of proteoliposomes is the big advancement of the method presented. In contrast to previous approaches more complex and medically relevant proteins can now be targeted, requiring of course the prior establishment of a reconstitution protocol yielding functional protein of choice in LUVs. Additionally, membrane proteins possessing large extra-membrane domains decrease the formation of proper SSMs. This has to be optimized for each new protein, for example by varying the CaCl_2 concentration.

The reconstitution ratio of the protein of interest has to be chosen carefully. The analysis of single protein events is desired and accomplishable using the here presented technique. The amount of reconstituted protein should therefore not exceed 1-2 functional protein units per pore-spanning membrane patch assuming an ideal reconstitution and that the membrane protein is stochastically distributed across the bilayer. Additionally the directionality of the protein after reconstitution should also be kept in mind, as it has not to be equal between both directionalities.

Finally once all these issues are carefully checked and optimized, none of the used substrates may display any unspecific membrane permeability of the pore-spanning membrane. Positively charged fluorophores, like most rhodamine-based dyes in the red spectral regime tend to quickly overcome the membrane barrier. Strong hydrophobic interactions can also lead to an unspecific attachment to the lipid bilayer. Both properties are not desired.

The study of ion channels in a qualitative manner is also imaginable. Screening for channel effectors using a binary Yes/No readout could be thought of using ion-sensitive dyes. The biggest obstacle here would be the establishment of an at least partly ion-retaining lipid bilayer. This might only be achievable via surface modification of the nanopore chip.

Disclosures

The authors declare no competing financial interests.

Acknowledgements

We thank Barbara Windschiegel for her help in establishing SOPs; Dennis Remme for his work on the NanoCalcFX software and Alina Kollmannsperger, Markus Braner and Milan Gerovac for helpful suggestions on the manuscript. The German-Israeli Project Cooperation (DIP) provided by the DFG and the Federal Ministry of Education and Research to R.T., as well as the Federal Ministry of Economics and Technology (ZIM R&D Project) to R.T. and Nanospot GmbH supported this work.

References

1. Yildirim, M.A., Goh, K.-I., Cusick, M. E., Barabási, A.-L., & Vidal, M. Drug-target network. *Nat. Biotechnol.* **25**, 1119 (2007).
2. Hamill, O. P., Marty, A., Neher, E., Sakmann, B., & Sigworth, F. Improved patch-clamp techniques for high-resolution current recording from cells and cell-free membrane patches. *Pflügers Arch.* **391**, 85-100 (1981).
3. Osaki, T., Suzuki, H., Le Pioufle, B., & Takeuchi, S. Multichannel simultaneous measurements of single-molecule translocation in α -hemolysin nanopore array. *Anal. Chem.* **81**, 9866-9870 (2009).
4. Carrillo, L. *et al.* High-resolution membrane capacitance measurements for studying endocytosis and exocytosis in yeast. *Traffic.* (2015).
5. Giacomini, K. M. *et al.* Membrane transporters in drug development. *Nat. Rev. Drug Discov.* **9**, 215-236 (2010).
6. Castell, O. K., Berridge, J., & Wallace, M. I. Quantification of membrane protein inhibition by optical ion flux in a droplet interface bilayer array. *Angew. Chem. Int. Ed.* **51**, 3134-3138 (2012).
7. Zollmann, T. *et al.* Single liposome analysis of peptide translocation by the ABC transporter TAPL. *Proc. Natl. Acad. Sci. U.S.A.* **112**, 2046-2051 (2015).
8. Tamm, L. K., & McConnell, H. M. Supported phospholipid bilayers. *Biophys. J.* **47**, 105-113 (1985).
9. Sackmann, E. Supported membranes: scientific and practical applications. *Science.* **271**, 43-48 (1996).
10. Castellana, E. T., & Cremer, P. S. Solid supported lipid bilayers: From biophysical studies to sensor design. *Surf. Sci. Rep.* **61**, 429-444 (2006).
11. Wagner, M. L., & Tamm, L. K. Tethered polymer-supported planar lipid bilayers for reconstitution of integral membrane proteins: silane-polyethyleneglycol-lipid as a cushion and covalent linker. *Biophys. J.* **79**, 1400-1414 (2000).
12. Naumann, C. A. *et al.* The polymer-supported phospholipid bilayer: tethering as a new approach to substrate-membrane stabilization. *Biomacromolecules* **3**, 27-35 (2002).
13. Weiskopf, D., Schmitt, E. K., Klühr, M. H., Dertinger, S. K., & Steinem, C. Micro-BLMs on highly ordered porous silicon substrates: Rupture process and lateral mobility. *Langmuir.* **23**, 9134-9139 (2007).
14. Watanabe, R. *et al.* Arrayed lipid bilayer chambers allow single-molecule analysis of membrane transporter activity. *Nat. Commun.* **5** (2014).
15. Stamou, D., Duschl, C., Delamarche, E., & Vogel, H. Self-Assembled Microarrays of Attoliter Molecular Vessels. *Angew. Chem. Int. Ed.* **115**, 5738-5741 (2003).
16. Lohr, C. *et al.* Single Liposomes Used to Study the Activity of Individual Transporters. *Biophysical Journal* **106**, 229a (2014).

17. Dunlop, J., Bowlby, M., Peri, R., Vasilyev, D., & Arias, R. High-throughput electrophysiology: an emerging paradigm for ion-channel screening and physiology. *Nat. Rev. Drug Discov.* **7**, 358-368 (2008).
18. Milligan, C. J. *et al.* Robotic multiwell planar patch-clamp for native and primary mammalian cells. *Nat. Protoc.* **4**, 244-255 (2009).
19. Soga, N., Watanabe, R., & Noji, H. Attolitre-sized lipid bilayer chamber array for rapid detection of single transporters. *Sci. Rep.* **5** (2015).
20. Kleefen, A. *et al.* Multiplexed parallel single transport recordings on nanopore arrays. *Nano Lett.* **10**, 5080-5087 (2010).
21. Wei, R., Gatterdam, V., Wieneke, R., Tampé, R., & Rant, U. Stochastic sensing of proteins with receptor-modified solid-state nanopores. *Nat. Nanotechnol.* **7**, 257-263 (2012).
22. Urban, M. *et al.* Highly parallel transport recordings on a membrane-on-nanopore chip at single molecule resolution. *Nano Lett.* **14**, 1674-1680 (2014).
23. Kusters, I., Van Oijen, A. M., & Driessen, A. J. Membrane-on-a-Chip: Microstructured Silicon/Silicon-Dioxide Chips for High-Throughput Screening of Membrane Transport and Viral Membrane Fusion. *ACS Nano*. **8**, 3380-3392 (2014).
24. Hansen, J. S., Thompson, J. R., Hélix-Nielsen, C., & Malmstadt, N. Lipid directed intrinsic membrane protein segregation. *J. Am. Chem. Soc.* **135**, 17294-17297 (2013).
25. Heinemann, F., & Schwille, P. Preparation of Micrometer-Sized Free-Standing Membranes. *ChemPhysChem*. **12**, 2568-2571 (2011).
26. Lazzara, T. D., Carnarius, C., Kocun, M., Janshoff, A., & Steinem, C. Separating attoliter-sized compartments using fluid pore-spanning lipid bilayers. *ACS nano*. **5**, 6935-6944 (2011).
27. Winterhalter, M. Black lipid membranes. *Curr. Opin. Colloid Interface Sci.* **5**, 250-255 (2000).
28. Koçer, A., Walko, M., & Feringa, B. L. Synthesis and utilization of reversible and irreversible light-activated nanovalves derived from the channel protein MscL. *Nat. Protoc.* **2**, 1426-1437 (2007).